Theoretical Study of 5-Aminolevulinic Acid Tautomerization: A Novel Self-Catalyzed Mechanism

Edvin Erdtman[†,‡] **and Leif A. Eriksson***[,†]

Department of Natural Sciences and Örebro Life Science Center, Örebro University, 701 82 Örebro, Sweden, and Modelling and Simulation Research Center, Örebro University, 701 82 Örebro, Sweden

Received: December 17, 2007; In Final Form: February 5, 2008

5-Aminolevulinic acid (5ALA) is the key synthetic building block in protoporphyrin IX (PpIX), the heme chromophore in mitochondria. In this study density functional theory calculations were performed on the tautomers of 5ALA and the tautomerization reaction mechanism from its enolic forms (5-amino-4-hydroxypent-3-enoic acid and 5-amino-4-hydroxypent-4-enoic acid) to the more stable 5ALA. The hydrated form 5-amino-4,4-dihydroxypentanoic acid was also studied. The lowest energy pathway of 5ALA tautomerization is by means of autocatalysis, in that an oxygen of the carboxylic group transfers the hydrogen atom as a "crane", with an activation energy of ∼15 kcal/mol. This should be compared to the barriers of about 35 kcal/mol for water assisted tautomerization, and 60 kcal/mol for direct hydrogen transfer. For hydration of 5ALA, the water catalyzed activation barrier is found to be ∼35 kcal/mol, approximately 5 kcal/mol lower than direct hydration.

1. Introduction

Keto−enol tautomerism reactions occur in organic compounds containing a carbonyl group (i.e., ketones or aldehydes). A proton or a hydrogen atom is moving from one of the α-carbons to the ketone oxygen atom forming an enol, with a hydroxyl group attached to an sp^2 hybridized carbon.

Tautomerization processes are important in many biological systems. For example the tautomerization of DNA bases may cause mutations.[1] In enzymatic mechanisms, otherwise unstable tautomeric forms can become stabilized in the active sites, thereby enabling reactions that otherwise would not be feasible. This has, for example, been one of the proposed enzymatic mechanisms of the enzyme porphobilinogen synthase (PBGS; EC 4.2.1.24), for which 5-aminolevulinic acid (5ALA) is the substrate.[2,3]

A large number of theoretical studies of tautomerization reactions are reported in the literature. An example is given by the ab initio studies of malonaldehyde.[4,5] In both these studies implicit water molecules were used to solvate the molecule. The use of two bridging waters and two solvating molecules was found to drastically reduce the activation energy of tautomerization to form the *Z* isomer compared to the use of only one bridging water molecule (from 26.2 to 5.8 kcal/mol). In the current work a dielectric continuum was instead used to model the solvent effect of water.

5ALA (Scheme 1) has gained much attention and several experimental and clinical studies thereof have been published during the past decade,[6] primarily due to its promising use as a prodrug in photodynamic therapy (PDT). Because 5ALA is the first precursor to heme and other porphyrin derivates, the light-harvesting molecule protoporphyrin IX (PpIX) can be accumulated in the cell by metabolism of 5ALA via a sequence of five enzymes (porphobilinogen synthase, porphobilinogen deaminase, uroporphyrinogen synthase, uroporphyrinogen decarboxylase and protoporphyrinogen IX oxidase).

SCHEME 1: Different Protonated States of 5ALA and Its Tautomers

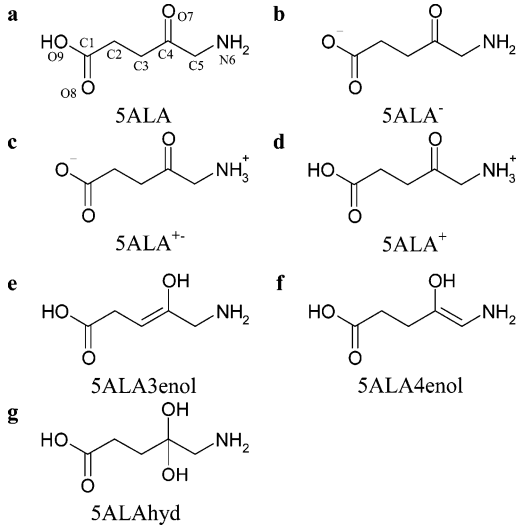

In some porphyric disorders (e.g., lead poisoning, acute intermittent porphyria (AIP), tyrosinosis) 5ALA is accumulated. In lead poisoning, PBGS is inhibited as a result of lead replacing the catalytic zinc ions in the active site. The accumulation of 5ALA also results in increased levels of its tautomers, which in its turn yields harmful oxyradicals.[7] Accordingly, it is important to study the tautomerization process of 5ALA and its stability in different environments. We have recently explored the properties of 5ALA and its methyl, ethyl and hexyl esters based on theoretical quantum chemical calculations (Scheme 1).[8] Our conclusions are that, using the previously determined value 267.68 kcal/mol for solvated protons,[9] the cationic forms of both 5ALA and its alkyl esters are the most stable forms in water. There is also a clear connection between the alkyl ester

* Corresponding author. E-mail: leif.eriksson@nat.oru.se.
† Department of Natural Sciences and Örebro Life Science Center.
‡ Modelling and Simulation Research Center.

10.1021/jp7118197 CCC: $40.75
Published on Web 04/17/2008

SCHEME 2: Tautomerism and Hydration of 5ALA

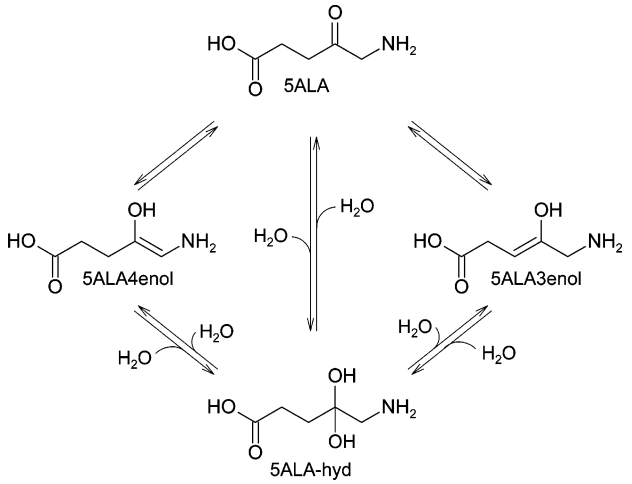

chain length and the energy gain of hydrolysis, where the hexyl ester is the most reactive of these three.

There are, besides the keto form, also four enol tautomers of 5ALA: 5ALA3enol and 5ALA4enol (depending on which carbons that form the double bond) each with *E* and *Z* stereoisomers (cf. Scheme 1).

Unless the enol is stabilized by other groups, enolic tautomers are generally less stable than the keto-forms. In the case of 5ALA the keto-form is in large excess. Jaffe et al. with found that the mol fraction of hydrated ALA (5ALAhyd) is 0.4% and 0.6%, using ^{13}C and ^{1}H NMR, respectively, in neutral pH and 37 °C.[10] The enolic forms were not detectable in their study, i.e., less than 0.3% of these were formed. Notable is that they found that 5ALA exists as dihydropyrazine (condensated 5ALA dimer formed in neutral and alkaline conditions[11]) in 4−7% depending of the concentration of 5ALA. Deuterium exchange rates indicate that the tautomerization is 4 times faster for the 4enol than the 3enol in phosphate buffer at pH 6.8. Jaffe et al. also compared 5ALA with the similar compounds 5-chlorolevulinic acid (5CLA) and Levulinic acid (LA).[10] The rate of tautomerization for 5CLA was concluded to be 3 times slower than 5ALA for 3enol but of the same order for the 4enol, whereas LA was more than 100 times slower than 5ALA. The use of phosphate buffer resulted in the fastest rates, indicating that the buffer molecules themselves could possibly be involved in the mechanism.

In the current work the tautomeric forms of 5ALA and its hydrated species, depicted in Scheme 2, were studied using hybrid density functional theory (DFT). We have explored the properties of different protonated and deprotonated forms of the enols and compared different mechanisms of the tautomerization process: direct transition, via an explicit water molecule, and self-catalyzation via the carboxylic acid part of the molecule. We have also examined if the hydrated form of 5ALA

	3enol E	3enol Z	4enol E	4enol Z
cation		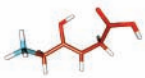	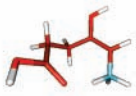	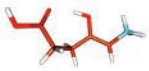
	$C\text{-}O_{enol}$ 1.371 C=C 1.343 $O\text{-}H_N$ 1.808	$C\text{-}O_{enol}$ 1.367 C=C 1.344 $O_{acid}\text{-}H_{Oenol}$ 1.720	$C\text{-}O_{enol}$ 1.358 C=C 1.343 $O\text{-}H_N$ 1.766	$C\text{-}O_{enol}$ 1.354 C=C 1.342 $O\text{-}H_{Oenol}$ 1.680
anion	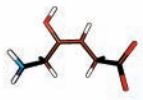		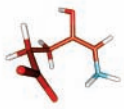	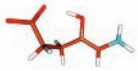
	$C\text{-}O_{enol}$ 1.386 C=C 1.344	$C\text{-}O_{enol}$ 1.368 C=C 1.350 $O_{acid}\text{-}H_{Oenol}$ 1.625	$C\text{-}O_{enol}$ 1.402 C=C 1.345 $O\text{-}H_N$ 2.069	$C\text{-}O_{enol}$ 1.382 C=C 1.347 $O_{acid}\text{-}H_{Oenol}$ 1.606
neutral	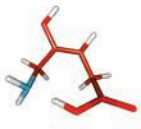	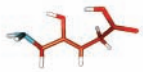	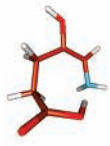	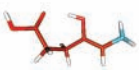
	$C\text{-}O_{enol}$ 1.374 C=C 1.344 $H_{Oacid}\text{-}N$ 1.553	$C\text{-}O_{enol}$ 1.380 C=C 1.340 $O_{enol}\text{-}H_{Oacid}$ 1.751	$C\text{-}O_{enol}$ 1.387 C=C 1.343 $H_{Oacid}\text{-}N$ 1.565	$C\text{-}O_{enol}$ 1.390 C=C 1.346 $O_{acid}\text{-}H_{Oenol}$ 1.790
zwitter		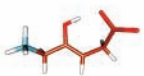		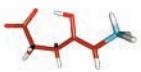
	$C\text{-}O_{enol}$ 1.376 C=C 1.343 $O_{acid}\text{-}H_N$ 1.518	$C\text{-}O_{enol}$ 1.362 C=C 1.347 $O_{acid}\text{-}H_{Oenol}$ 1.499	$C\text{-}O_{enol}$ 1.366 C=C 1.342 $O_{acid}\text{-}H_N$ 1.459	$C\text{-}O_{enol}$ 1.339 C=C 1.348 $O_{acid}\text{-}H_{Oenol}$ 1.388

Figure 1. Optimized 5ALA enols in different protonation states and symmetries.

(5ALAhyd, cf. Scheme 1) may be involved in the tautomeric transition (Scheme 2).

2. Computational Models and Methods

All optimizations were performed using the hybrid DFT functional B3LYP,[12−14] in conjunction with the 6-31+G(d,p) basis set. The optimizations were generally carried out in bulk solvent using the integral equation formalism of the polarizable continuum model (IEFPCM).[15,16] In the PCM calculations, water was used as solvent, through the value $\epsilon = 78.4$ of the dielectric constant. To investigate how the different species behave in a highly nonpolar environment such as lipid membranes, single point IEFPCM calculations with $\epsilon = 4.0$ were also carried out. Frequency calculations were performed at 298.15 K, to obtain zero-point vibrational energies (ZPE) and thermal corrections to the Gibbs free energies and the enthalpy. Proton affinities were determined as the difference between the enthalpy corrected internal energies of the protonated and non-protonated forms, using the definition $PA = -\Delta H_{protonation}$. In reactions involving solvated protons, the previously established solvation energy of H^+, 267.68 kcal/mol,[9] was employed to obtain reaction free energies. The accuracy of gradient corrected DFT for the calculations of proton affinities is well studied, and generally lies within 1−7 kcal/mol of experimental data.[17,18] All calculations were performed using the GAUSSIAN 03 program.[19]

3. Results

3.1. Structures and Free Energies. The optimized structures of the enols are different depending on their symmetry and protonation (cf. Figure 1). The enols with *E* symmetry generally form a hydrogen bond between the acid- and the amino group (1.46−2.07 Å), except for the anion where no intramolecular hydrogen bond is formed. The hydrogen bond is considerably shorter for the neutral and zwitterionic systems (∼1.5 Å) compared to the cation. For the system of *Z* symmetry, hydrogen bonds are instead formed between the enol and acid groups (1.39−1.79 Å).

Comparing with the data from our former study of 5ALA using the same computational method,[8] the current results show that independently of protonation state, all the enols are less stable than the corresponding keto-form (5ALA). Figure 2 shows the ΔG for either of the following reactions:

$$5ALA^+(aq) \rightarrow 5ALA(enol)^n + (1 - n)H^+(aq)$$

$$5ALA^+(aq) + H_2O(aq) \rightarrow 5ALAhyd^n + (1 - n)H^+(aq)$$

where *n* is the total charge of the molecule. Reaction free energies for conversion between the various forms are also listed in Table 1.

The graph in Figure 2 shows no obvious trends regarding the relative stabilities of the 3enol vs the 4enol tautomers. For the 4enols the *Z* symmetry is more stable than *E*. For the 3enols it is dependent on the protonation form. The anions have a more stable *Z* than *E* confomer which can be rationalized in terms of the hydrogen bond formed, in those cases between the enolic OH and one of the carboxylic oxygen atoms. The opposite is true for the neutral forms, where the stronger hydrogen bond between the carboxylic group and the amino group is formed. The zwitterionic and cationic species, which all form internal hydrogen bonds, show no major differences in energy. The enols are following the same order of stability with respect to the protonation state as 5ALA both in water and in lipid phase, with the cation being the most stable form in water and the neutral species in lipid phase. The only exception to the trend is the 3enol *Z* form in aqueous solution, where the zwitterion is more stable than the neutral species, albeit very close in energy (1 kcal/mol).

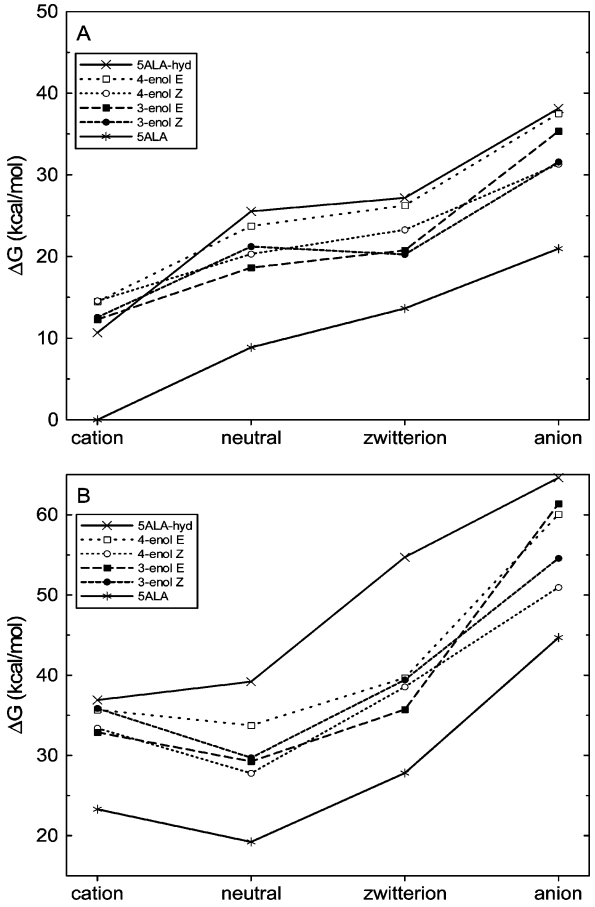

Figure 2. Mass balanced relative free energies (kcal/mol) in (a) water and (b) lipid environment. The energy of $5ALA^+(aq) + H_2O(aq)$ is set to zero. The free energy of a proton is used according to ref 9.

The hydrated form of 5ALA (5ALAhyd) is less stable than the enols except for the cationic form in aqueous solution in which case this is more stable than any of the enols. The cationic $5ALAhyd^+$ is the most stable of the hydrated species also in lipid environment. The ΔG_{aq}^{298} of hydration of $5ALA^+$ is +10.7 kcal/mol.

3.2. Proton Affinities. The proton affinities (PA), obtained in water and lipid phase are given in Figure 3 (table included in Supporting Information). As was noted also for 5ALA,[8] the PA of the anions in lipid environment are higher than in water phase for all enols, and the oxygen atom is more easily protonated than the nitrogen atom in lipid phase. The neutral and the zwitterionic compounds are more easily protonated in water, as seen also for 5ALA.

These results are expected because the neutral form should be the most stable in the nonpolar lipid phase, whereas the polar dielectric water model stabilizes the charged species relative to the neutral ones. Overall, the species of *E* symmetry have slightly higher proton affinities than those of *Z* symmetry, in particular for the anions.

The hydrated form behaves somewhat differently. Both the neutral and the zwitterionic hydrated 5ALA are easier protonated than either the enols or 5ALA. Notable is also that the zwitterionic form of 5ALAhyd is more readily protonated in lipid phase than the other compounds, leading to a very small difference between protonation in water or lipid. The differences

TABLE 1: Reaction Free Energies (ΔG, kcal/mol) at 298.15 K (All Systems Optimized in Aqueous Solution)

reactant(s)	product(s)	water	lipid
$5ALA^+$	$5ALA + H^+$	8.36	−3.15[a]
5ALA	$5ALA^- + H^+$	13.09	25.34[a]
5ALA	$5ALA^{+-}$	4.78	8.58
$5ALA^{+-}$	5ALA3enol *Z*	7.57	1.91
$5ALA^{+-}$	5ALA3enol *E*	4.98	1.44
$5ALA^{+-}$	$5ALA3enol^{+-}$ *Z*	6.60	11.62
$5ALA^{+-}$	$5ALA3enol^{+-}$ *E*	7.10	7.92
5ALA3enol *Z*	5ALA3enol *E*	−2.59	−0.46
$5ALA3enol^{+-}$ *Z*	$5ALA3enol^{+-}$ *E*	0.50	−3.70
$5ALA3enol^{+}$ *Z*	$5ALA3enol^{+}$ *E*	−0.26	−2.99
$5ALA3enol^{-}$ *Z*	$5ALA3enol^{-}$ *E*	3.76	6.80
$5ALA3enol^{+}$ *Z*	5ALA3enol *Z* + H^+	8.67	−6.16[a]
$5ALA3enol^{+}$ *E*	5ALA3enol *E* + H^+	6.34	−3.63[a]
5ALA3enol *Z*	$5ALA3enol^{-}$ *Z* + H^+	10.36	24.86[a]
5ALA3enol *Z*	$5ALA3enol^{+-}$ *Z*	−0.97	9.71
5ALA3enol *E*	$5ALA3enol^{+-}$ *E*	2.12	6.47
$5ALA^{+-}$	5ALA4enol *Z*	6.66	−0.02
$5ALA^{+-}$	5ALA4enol *E*	10.34	4.58
$5ALA^{+-}$	$5ALA4enol^{+-}$ *Z*	9.61	10.74
$5ALA^{+-}$	$5ALA4enol^{+-}$ *E*	12.59	11.86
5ALA4enol *Z*	5ALA4enol *E*	3.68	4.60
$5ALA4enol^{+-}$ *Z*	$5ALA4enol^{+-}$ *E*	2.98	1.13
$5ALA4enol^{+}$ *Z*	$5ALA4enol^{+}$ *E*	−0.09	2.30
$5ALA4enol^{-}$ *Z*	$5ALA4enol^{-}$ *E*	6.21	9.12
$5ALA4enol^{+}$ *Z*	5ALA4enol *Z* + H^+	5.74	−5.60[a]
$5ALA4enol^{+}$ *E*	5ALA4enol *E* + H^+	9.51	−3.31[a]
5ALA4enol *Z*	$5ALA4enol^{-}$ *Z* + H^+	10.99	23.15[a]
5ALA4enol *Z*	$5ALA4enol^{+-}$ *Z*	2.95	10.75
5ALA4enol *E*	$5ALA4enol^{+-}$ *E*	2.25	7.28
$5ALA3enol^{+-}$ *Z*	$5ALA4enol^{+-}$ *Z*	3.01	3.95
$5ALA3enol^{+-}$ *E*	$5ALA4enol^{+-}$ *E*	5.49	−0.88
5ALA + H_2O	5ALA-hyd	16.66	19.96
$5ALA^{+-}$ + H_2O	$5ALA\text{-}hyd^{+-}$	13.53	24.02
$5ALA^{+}$ + H_2O	$5ALA\text{-}hyd^{+}$	10.67	13.62
$5ALA^{-}$ + H_2O	$5ALA\text{-}hyd^{-}$	17.17	19.92
$5ALA3enol^{+-}$ *E* + H_2O	$5ALA\text{-}hyd^{+-}$	6.42	18.99
$5ALA3enol^{+-}$ *Z* + H_2O	$5ALA\text{-}hyd^{+-}$	6.93	15.29
$5ALA4enol^{+-}$ *E* + H_2O	$5ALA\text{-}hyd^{+-}$	0.94	15.04
$5ALA4enol^{+-}$ *Z* + H_2O	$5ALA\text{-}hyd^{+-}$	3.92	16.17

[a] Free energy of the proton in water is used.[9]

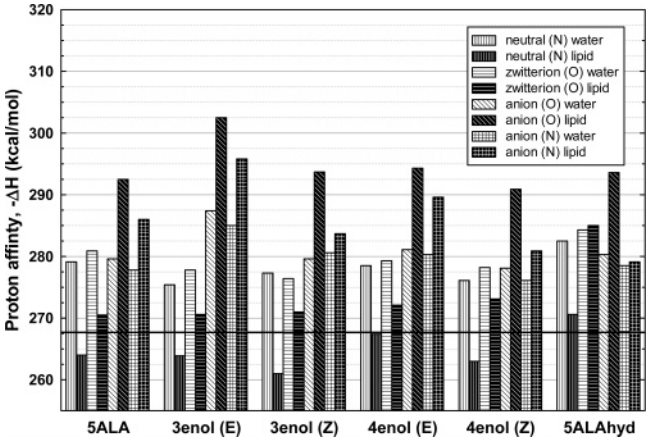

Figure 3. Proton affinities (kcal/mol) of 5ALA-enols and 5ALAhyd compared with 5ALA. The line across the chart shows the proton energy used for the ΔG calculations.[9]

in PA between water and lipid phases at the nitrogen of the 5ALAhyd anion is also very small.

3.3. Tautomerization Mechanism. We have studied the tautomerization of aminolevulinic acid from the zwitterionic 3enol and 4enol *Z* confomers ($5ALA3enol^{+-}$ and $5ALA4enol^{+-}$) to the zwitterionic $5ALA^{+-}$.

Three different mechanisms have been explored for each of the two tautomeric transition reactions. For all of them the

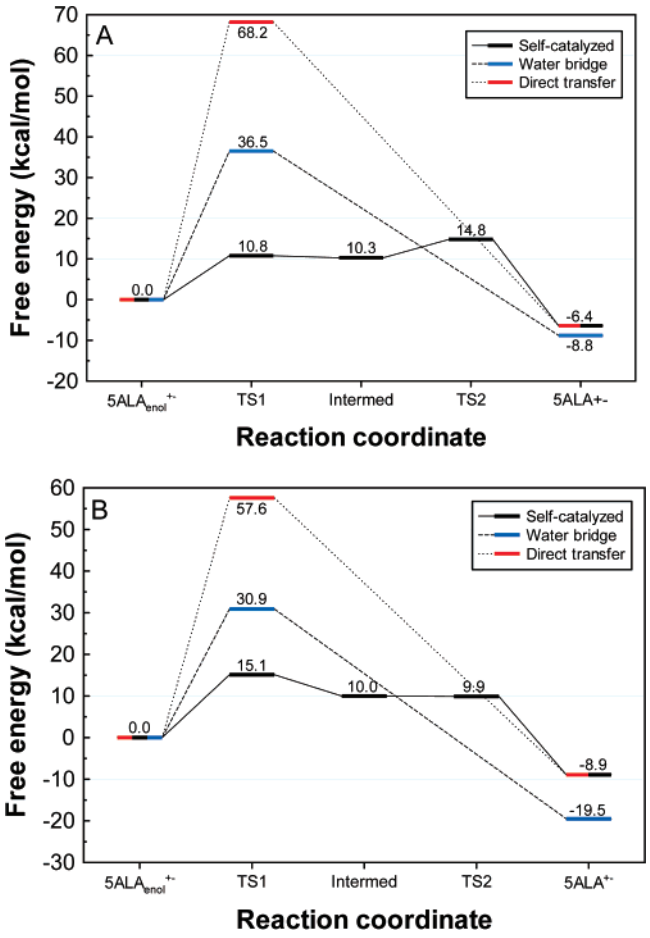

Figure 4. Reaction free energies of (a) $5ALA3enol^{+-}$ and (b) $5ALA4enol^{+-}$ (kcal/mol).

Mulliken charge of the transferred hydrogen atom does not change appreciably during the tautomerization, which indicates that the tautomerization of $5ALA^{+-}$ is a hydrogen transfer, i.e., that the proton and the electron are transferred simultaneously.

The first mechanism is the direct transfer of the hydrogen from O7 to either C3 or C5 (Figures 5a and 6a). The transition state forms a 4-membered ring and is, therefore, unstable due to high strain. The activation energies (E_a) for both the 3enol and the 4enol are hence very high: 68 and 58 kcal/mol, respectively (cf. Figure 4).

The second mechanism proceeds via a bridging water molecule (Figures 5b−d and 6b−d). Here a more stable 6-membered ring is formed in the transition state. The water in the TS of the 3enol (Figure 5c) resembles a bridging hydronium ion, from which a reaction in either direction leads to bond formation. The 4enol on the other hand, has what is better described as a bridging water molecule in the TS, with the water acting as a H-atom shuffle, forming one O−H bond as the other is broken. The activation energies of these reactions are almost half of those for the direct mechanism: 37 and 31 kcal/mol, respectively.

These are, however, not the most favored mechanisms. It was found that atom O9 in the carboxylic acid group may also act as a 'crane' transferring the hydrogen atom from O7 to either C3 or C5 (Figures 5e−i and 6e−i). The two transition states of the 3enol form a 7-membered and a 5-membered ring, respectively, and the 4enol forms 7-membered rings in both transition states. For both the 3enol and the 4enol this mechanism has the lowest activation free energy.

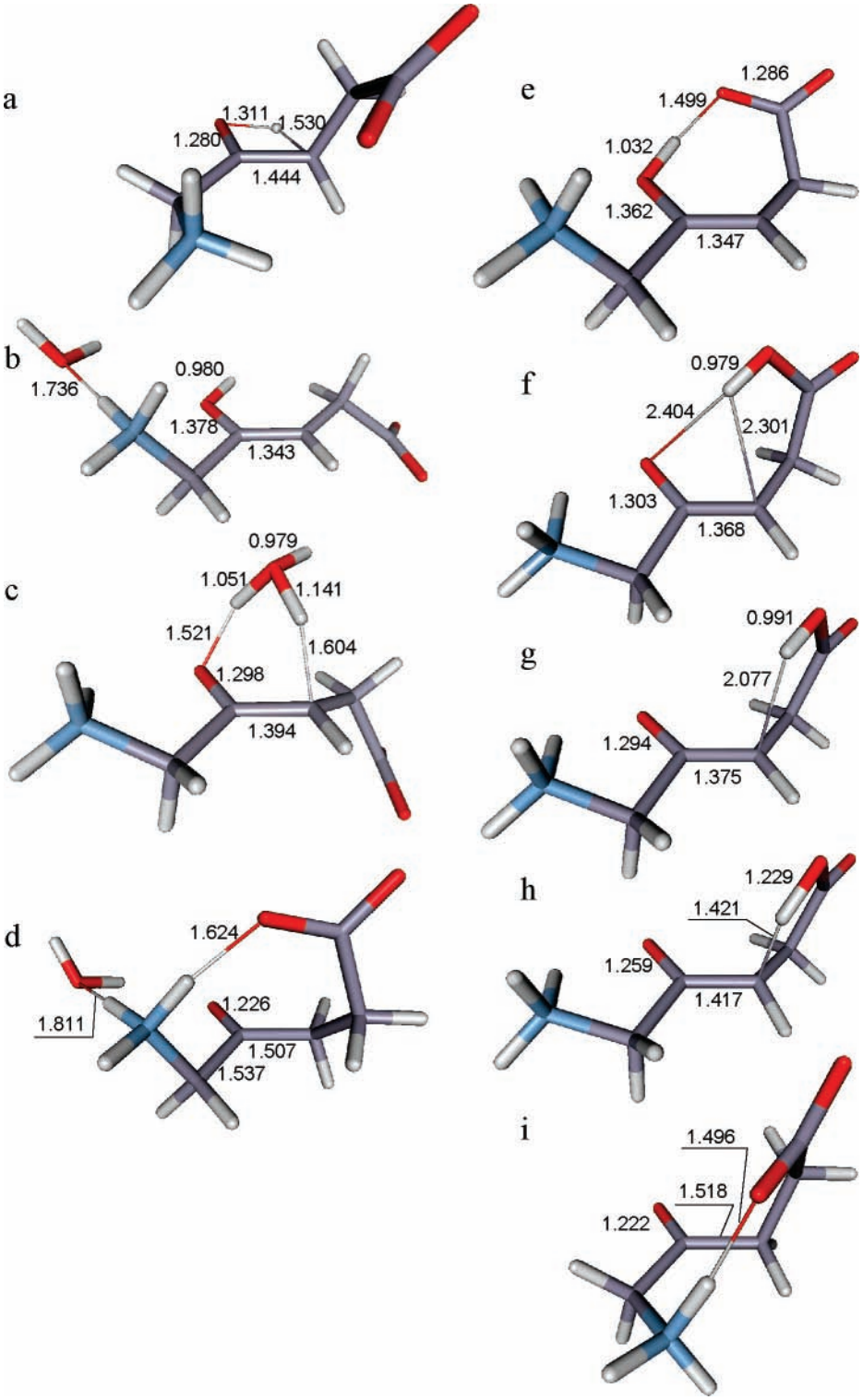

Figure 5. Optimized structures of 3enol tautomerization: (a) direct transfer; (b)−(d) water catalyzed; (e)−(i) self-catalyzed mechanism. Structures: (a) $TS^{direct\ transfer}$; (b) $5ALA3enol^{+-} + H_2O$; (c) $TS^{water\ cat}$; (d) $5ALA^{+-} + H_2O$; (e) $5ALA3enol^{+-}$; (f) $TS1^{self-cat}$; (g) $IM^{self-cat}$; (h) $TS2^{self-cat}$; (i) $5ALA^{+-}$.

The 3enol calculations show that the self-catalyzed mechanism has two transition states. The first (TS1) occurs with the hydrogen bonded to the carboxylic oxygen, with an imaginary frequency corresponding to a motion of the hydrogen atom between O7 and C3. $\Delta G^{\ddagger}$ for TS1 is 10.8 kcal/mol. An intermediate structure is found at 10.3 kcal/mol − a local minimum before the hydrogen is transferred to the carbon atom. The second TS, 14.8 kcal/mol above the initial reactant, represents a barrier of 4.5 kcal/mol to transfer the hydrogen to the carbon atom. The 4enol self-catalyzed mechanism also has two transition states. In this case, however, the highest activation energy barrier is found at the first transition state: 15.1 kcal/mol. This transition state is closer to the reactant than the first TS of the 3enol mechansim. The intermediate structure is closer to the product than what is the case for the 3enol intermediate (H−C bond length is 1.894 Å, compared to 2.077 Å for the 3enol). The second transition state involves the transfer of the hydrogen from O9 at the carboxylic group to C5. In Figure 4b,

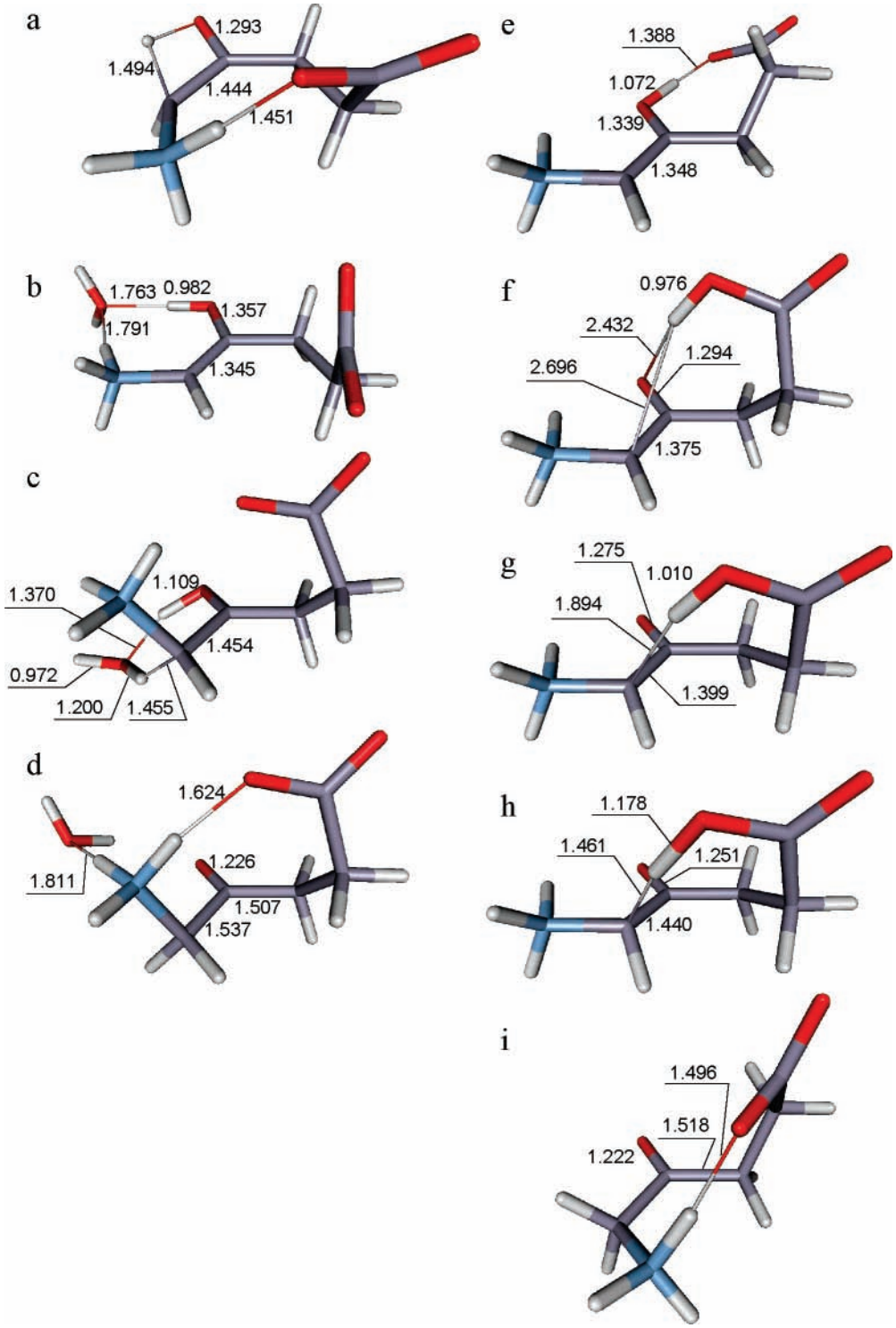

Figure 6. Optimized structures of 4enol tautomerization: (a) direct transfer; (b)−(d) water catalyzed; (e)−(i) self-catalyzed mechanism. Structures: (a) $TS^{direct\ transfer}$; (b) $5ALA4enol^{+-} + H_2O$; (c) $TS^{water\ cat}$; (d) $5ALA^{+-} + H_2O$; (e) $5ALA4enol^{+-}$; (f) $TS1^{self-cat}$; (g) $IM^{self-cat}$; (h) $TS2^{self-cat}$; (i) $5ALA^{+-}$.

TS2 appears no to be a real TS, in that the energy level of the intermediate is slightly higher than the energy of TS2. In fact the energies are very close, and by adding the free energy corrections the TS becomes 0.1 kcal/mol lower in energy than the intermediate.

3.4. Hydration Mechanism. The mechanism of hydration of the 5ALA zwitterion was also explored (cf. Scheme 2). As this also involves hydrogenation of the keto-oxygen, two mechanisms were investigated, involving either direct transfer of hydrogen from the adding water molecule (Figure 7a−c), or involving a second bridging water molecule (Figure 7d−f).

The two transition states are highly similar in the local structures at the adding oxygen and hydrogen; using an additional bridging water only extends the C−O and O−H distances with a few hundreds of an Ångström.

Energetically, the noncatalyzed hydration has an activation energy of 40 kcal/mol, whereas in presence of a bridging water

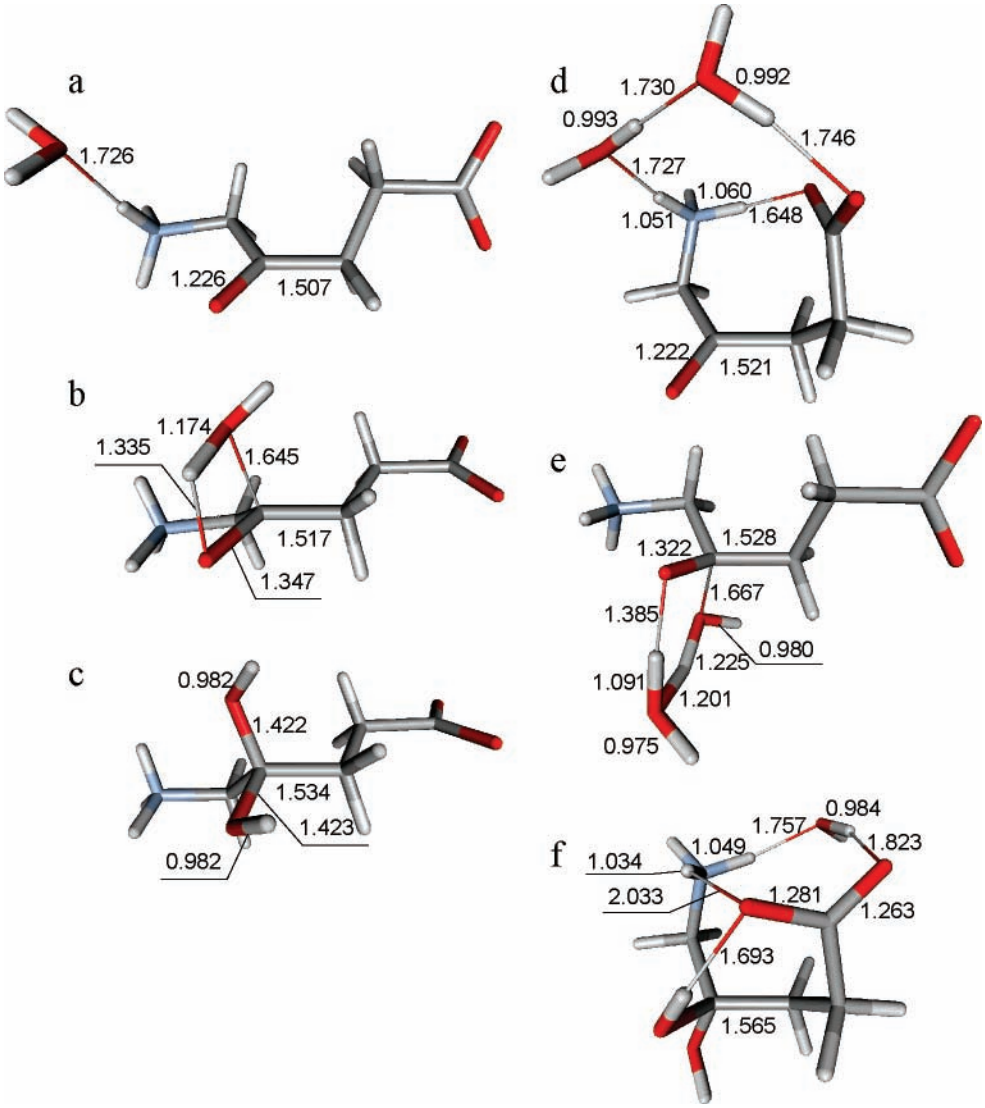

Figure 7. Optimized structures of hydration reaction of 5ALA: (a)−(c) uncatalyzed; (d)−(f) water catalyzed mechanism. Structures: (a) $5ALA^{+-}$ + H_2O; (b) TS^{un-cat}; (c) $5ALAhyd^{+-}$; (d) $5ALA^{+-}$ + 2 H_2O; (e) $TS^{water\ cat}$; (f) $5ALAhyd^{+-}$ + H_2O.

molecule the activation energy is reduced to 35 kcal/mol. For this reaction the addition of an explicit water molecule hence does not provide an as significant increase in reaction rate as seen for the tautomerization reactions. The hydrated forms lie 10−17 kcal/mol above the initial reactants, slightly higher than the enolic species.

4. Conclusions

Several possible mechanisms of tautomerization of 5ALA have been explored. The tautomerization is found to occur through hydrogen transfer, where the most favorable reaction mechanism proceeds through self-catalysis. The carboxylic group is playing a key role in this mechanism, as it actively transfers the hydrogen atom from the hydroxyl group to the carbon, like a "crane". The energy barriers are around 15 kcal/mol, which is half the activation energy required for the tautomerization reaction to proceed via a bridging water molecule. The activation energies of the different enol forms are quite similar, even though the transition states are slightly different. The results cannot fully explain the fact that the 4enol tautomerization is 4 times faster than the 3enol tautomerization,[10] because the activation energies determined herein are highly similar. The 4enol is, however, slightly more thermodynamically stable than the 3enol.

According to our calculations the hydrated form of 5ALA is both thermodynamically relatively unstable and the activation energy of the hydration is furthermore very high (∼35 kcal/mol) even when involving a bridging water molecule in the mechanism. Further elucidation of the explicit mechanism will require a more extended model, presumably including quantum dynamics, and with several solvation shells.

Acknowledgment. The faculty of Science and technology of Örebro University and the Swedish science research council are gratefully acknowledged for financial support. We also acknowledge the National Supercomputer Centre (NSC) in Linköping for generous grants of computing time.

Supporting Information Available: Calculated proton affinities and optimized geometric structures. This information is available free of charge via the Internet at http://pubs.acs.org

References and Notes

(1) Watson, J. D.; Crick, F. H. C. *Nature* **1953**, *171*, 964.
(2) Goodwin, C. E.; Leeper, F. J. *Org. Biomol. Chem.* **2003**, *1*, 1443.
(3) Jordan, P. M. *Biosynthesis of Tetrapyrroles*; Elsevier: Amsterdam 1991.
(4) Yamabe, S.; Tsuchida, N.; Miyajima, K. *J. Phys. Chem. A* **2004**, *108*, 2750.

(5) Freitag, M. A.; Pruden, T. L.; Moody, D. R.; Parker, J. T.; Fallet, M. *J. Phys. Chem. A* **2007**, *111*, 1659.

(6) See Baumgartner, R.; Krammer, B.; Pottier, R.; Stepp, H. *Photodynamic Therapy with ALA*; RSC Publishing: London, 2006 (see also references therein).

(7) Bechara, E. J. H. *Braz. J. Med. Biol. Res.* **1996**, *29*, 841.

(8) Erdtman, E.; Eriksson, L. A. *Chem. Phys. Lett.* **2007**, *434*, 101.

(9) Llano, J.; Eriksson, L. A. *J. Chem. Phys.* **2002**, *117*, 10193.

(10) Jaffe, E. K.; Rajagopalan, J. S. *Bioorg. Chem.* **1990**, *18*, 381.

(11) Bunke, A.; Zerbe, O.; Schmid, H.; Burmeister, G.; Merkle, H. P.; Gander, B. *J. Pharm. Sci.* **2000**, *89*, 1335.

(12) Becke, A. D. *J. Chem. Phys.* **1993**, *98*, 5648.

(13) Lee, C. T.; Yang, W. T.; Parr, R. G. *Phys. Rev. B* **1988**, *37*, 785.

(14) Stephens, P. J.; Devlin, F. J.; Chabalowski, C. F.; Frisch, M. J. *J. Phys. Chem.* **1994**, *98*, 11623.

(15) Cancès, E.; Mennucci, B. *J. Chem. Phys.* **2001**, *114*, 4744.

(16) Cancès, E.; Mennucci, B.; Tomasi, J. *J. Chem. Phys.* **1997**, *107*, 3032.

(17) Fitzgerald, G.; Andzelm, J. *J. Phys. Chem.* **1991**, *95*, 10531.

(18) Topol, I. A.; Burt, S. K.; Toscano, M.; Russo, N. *J. Mol. Struct. (THEOCHEM)* **1998**, *430*, 41.

(19) Frisch, M. J.; Trucks, G. W.; Schlegel, H. B.; Scuseria, G. E.; Robb, M. A.; Cheeseman, J. R., Jr.; J. A. M.; Vreven, T.; Kudin, K. N.; Burant, J. C.; Millam, J. M.; Iyengar, S. S.; Tomasi, J.; Barone, V.; Mennucci, B.; Cossi, M.; Scalmani, G.; Rega, N.; Petersson, G. A.; Nakatsuji, H.; Hada, M.; Ehara, M.; Toyota, K.; Fukuda, R.; Hasegawa, J.; Ishida, M.; Nakajima, T.; Honda, Y.; Kitao, O.; Nakai, H.; Klene, M.; Li, X.; Knox, J. E.; Hratchian, H. P.; Cross, J. B.; Adamo, C.; Jaramillo, J.; Gomperts, R.; Stratmann, R. E.; Yazyev, O.; Austin, A. J.; Cammi, R.; Pomelli, C.; Ochterski, J. W.; Ayala, P. Y.; Morokuma, K.; Voth, G. A.; Salvador, P.; Dannenberg, J. J.; Zakrzewski, V. G.; Dapprich, S.; Daniels, A. D.; Strain, M. C.; Farkas, O.; Malick, D. K.; Rabuck, A. D.; Raghavachari, K.; Foresman, J. B.; Ortiz, J. V.; Cui, Q.; Baboul, A. G.; Clifford, S.; Cioslowski, J.; Stefanov, B. B.; Liu, G.; Liashenko, A.; Piskorz, P.; Komaromi, I.; Martin, R. L.; Fox, D. J.; Keith, T.; Al-Laham, M. A.; Peng, C. Y.; Nanayakkara, A.; Challacombe, M.; Gill, P. M. W.; Johnson, B.; Chen, W.; Wong, M. W.; Gonzalez, C.; Pople, J. A. *Gaussian 03*, revision B.02/C.02; Gaussian, Inc.: Pittsburgh, PA, 2003.